Magnetic Force Microscopy Characterization of Heat and Current Treated $Fe_{40}Ni_{38}Mo_4B_{18}$ Amorphous Ribbons

Ignacio García[a,b], Nuria Iturriza[a], Juan José del Val[b], Hans Grande[a], José A. Pomposo[d], Julián González[b]

[a] New Materials Department, Cidetec/Centre for Electrochemical Technologies, P° Miramón, E-20009 Donostia-San Sebastián, Spain. [b] Department of Materials Physics, Faculty of Chemistry, University of the Basque Country, P° Manuel de Lardizabal 3, E-20018 Donostia-San Sebastián, Spain. [c] CIC nanoGUNE Consolider, Paseo Mikeletegi 56, E-20009 Donostia-San Sebastián, Spain. [d] Donostia International Physics Center (DIPC), Paseo Manuel de Lardizabal 4, 20018 San Sebastián, Spain

ABSTRACT: The domain structure of a magnetostrictive $Fe_{40}Ni_{38}Mo_4B_{18}$ amorphous ribbon has been studied using magnetic force microscopy (MFM) at room temperature. First, the evolution of the magnetic domain patterns as a function of the annealing temperature has been investigated. In samples heat treated at 250 and 450 °C for 1 h, a transformation from 90° to 180° domain wall has been clearly observed, while the sample heat treated at 700 °C for 1 h showed a magnetic phase fixed by the crystalline anisotropy. Additionally, the evolution of the magnetic domain structure by applying a DC current was recorded by the MFM technique. For current annealed samples at 1 A for 1, 30 and 60 min, a transformation between different domain patterns has been observed. Finally, in samples treated by the current annealing method under simultaneous stress, an increase of the annealing time gives rise to a different magnetic structure arising from the development of transverse magnetic anisotropy.

Keywords: MFM; Amorphous ribbon; Domain pattern; Current annealing

1. Introduction.

The domain structure in metallic glasses is mainly fixed by the magnetoelastic anisotropies arising from the internal stresses introduced during the fabrication process. As a consequence, in Fe-rich amorphous alloys exhibiting high value of saturation constant the magnetization direction is oriented parallel to the ribbon axis plane,

corresponding to the region of the material where the internal stresses are of tensile nature. However, when the regions where the internal stress is of compressive character exist and when value of the saturation of magnetostriction is high the so-called "maze-domains", or islands, where the magnetization is oriented perpendicular to the ribbon plane, appear. This is due to the overcoming of demagnetizing effects [1,2] in these islands by the magnetoelastic anisotropy. Thus, the appearance of the domain structure is related to the aforementioned magnetization direction.

In order to improve the soft magnetic properties of Fe-rich amorphous alloys (positive magnetostriction) these materials are generally treated employing different annealing treatments. These treatments are able both to relax the internal stresses [3-6] generated in the production process and to induce magnetic anisotropies improving the magnetic behavior of the soft magnetic material. [7-9] The conventional method carried out is placing the sample inside a furnace with an inert atmosphere, which is provided to prevent the undesirable oxidation of the sample. Another type of annealing which has become successful due to its simplicity is called current annealing. [10-13] It is based on the Joule heating effect when an electric current flows along the ribbon axis, requiring shorter annealing time to get the desirable temperature when compared to the conventional method using a furnace.

In this sense, the amorphous alloy of composition $Fe_{40}Ni_{40}B_{20}$ has largely attracted considerable attention owing to its attractive soft magnetic behavior and mechanical properties. [14,15]In addition, this composition is one of easiest to produce as amorphous alloy by the melt-spinning technique. As stated before, nanocrystallization by means of thermal treatments of Fe-rich amorphous alloys leads to an improvement of the soft magnetic character. In the case of this amorphous alloy, the thermal treatment at high temperatures produces products which are generally large eutectic crystals. [15] However, nanocrystalline morphology would be more favorable for obtaining better soft magnetic properties, since the microstructure of the nanocrystals in an amorphous matrix gives rise to superior soft magnetic behavior compared to the amorphous counterpart. [16,17] Consequently, to promote the nanocrystallization process the addition of Mo has been found to be very attractive, [18,19] because it is known that Mo has a strong influence on the crystallization mechanisms, leading to a microstructure similar to that required by the Herzer model of soft nanocrystalline alloys. [17]

Magnetic force microscopy (MFM) is a useful technique to get information about local magnetic domains structure of mainly surface character. Pioneering work for the use of MFM was carried out in thin films by Rugar et al. [20] and in amorphous ribbons by Suzuki et al. [21,22]

Magnetic domain characterization in soft magnetic samples using the MFM technique is always challenging, requiring a very accurate adjustment of the configuration parameters. In spite of these inherent difficulties, MFM provides useful information to complete the magnetic characterization performed by standard macroscopic methods. In addition, in some nanometric magnetic structures [23,24] the MFM technique is the unique tool which provides magnetic phase images.

In previous works, MFM technique was used for morphological characterization of $Fe_{40}Ni_{38}Mo_4B_{18}$ ribbons. In both references it was reported MFM studies in this attractive alloy involves to several treatments such as annealing at different temperatures [25] and laser irradiation. [26] In this work, we report on magnetic domain structure evolution (as recorded by MFM) of amorphous ribbons of $Fe_{40}Ni_{38}Mo_4B_{18}$ before and after carrying out several annealing procedures: annealing at different temperatures under argon atmosphere; annealing by Joule heating at different electrical current intensities and using different treatment times and, finally, annealing under simultaneous current and mechanical stress.

2. Experimental section.

Amorphous ribbons of nominal composition $Fe_{40}Ni_{38}Mo_4B_{18}$ (trademark *Metglas* 2826MB) exhibiting quite large positive magnetostriction ($\lambda_s \approx 12\times10^{-6}$) were supplied by Metglas Corporation. Samples of thickness 32 μm, width 12 mm and length 12 cm and which were cleaned superficially employing ethanol have been employed in this work. Some of the samples were sealed inside alumina tubes in argon atmosphere for heat treatment at different temperatures (250, 450 and 700 °C) for 1 h, at 100 °C/min heating rate. Current annealing treatment was carried out in air atmosphere. The above temperatures were selected based on previously reported differential scanning calorimetry (DSC) measurements of Metglas 2826MB [18,19,27] showing two phase

transformation peaks at around 420 and 525 °C. The first one (420 °C) is related to the formation of $(FeNiMo)_{23}B_6$ crystalline phase embedded in the amorphous matrix, while the second one (525 °C) is related to the formation of the bcc-(Fe,Ni) ferromagnetic phase. Depending on the heating rate, the crystallization peaks move to higher temperatures. At 40 °C/min, the crystallization peaks are placed at around 442 and 550 °C as reported by Srivastava et al. [28] Other samples were annealed using the Joule heating technique, by flowing a DC electric current through its longitudinal direction at different current intensities and varying time. Also some samples were annealed by using a combined current and stress treatment. Stress annealing was performed using a weight failed in each extreme of the ribbon, and compression treatment was carried out by bending the ribbon.

Magnetic phase images of as-cast and annealed samples were obtained, at room temperature, using scanning probe microscope (Molecular Imaging´s PicoScan) and tips covered with CoCr supplied by MikroMasch (NSC35/Co–Cr). Cantilever (130 μm length) having a tip nominal radius of curvature of 90 nm and resonance frequency around 150 kHz were used. The tips were magnetized in such a way that the tip moment was approximately perpendicular to the plane of the surface sample. Typical lift height was of the order of 150 nm and was properly adjusted to give better contrast.

3. Results and discussion.

3.1. Magnetic domains configuration in conventional thermal treated samples.

Figure 1 shows topography and MFM images of $Fe_{40}Ni_{38}Mo_4B_{18}$ ribbon as was received. $Fe_{40}Ni_{38}Mo_4B_{18}$ amorphous ribbons treated in a furnace at 250 °C showed a *"flower"* shape magnetic domains configuration. The presence of easy axes which are normal to the ribbon plane is observed after 90° domain walls take a *"flower"* pattern configuration, which could represent the interaction with the surface of two 90° walls separating domains through the thickness and width directions as a consequence of the complex internal stresses in these regions of compressive nature [29] such as those shown in **Figure 1.** The traces of these walls on the ribbon surface appear to be generally oblique to both the ribbon length and the ribbon wide (surface ribbon). Where this oblique orientation alternates rapidly, the walls take on a *flower* appearance. These complex patterns are seen when the normal anisotropy becomes large (in competition

with the strong demagnetizing effect in this direction) and can be believed to represent further subdivision of the closure domains. It should be noted that maze-domains present in the as-cast state (as a consequence of the large positive magnetostriction and compressive stresses) are not observed. Therefore, the thermal treatment at this temperature produces a drastic decrease of the internal stresses via structural relaxation. The oblique orientation of the domain wall projections on the surface alternates rapidly generating a *zigzag* domain configuration in the surface. The explanation for the presence of these *flower* domains in noncrystalline materials is understood because they appear to decrease the total energy lengthening the walls, thus separating magnetic poles that result from the head-to-head orientation.

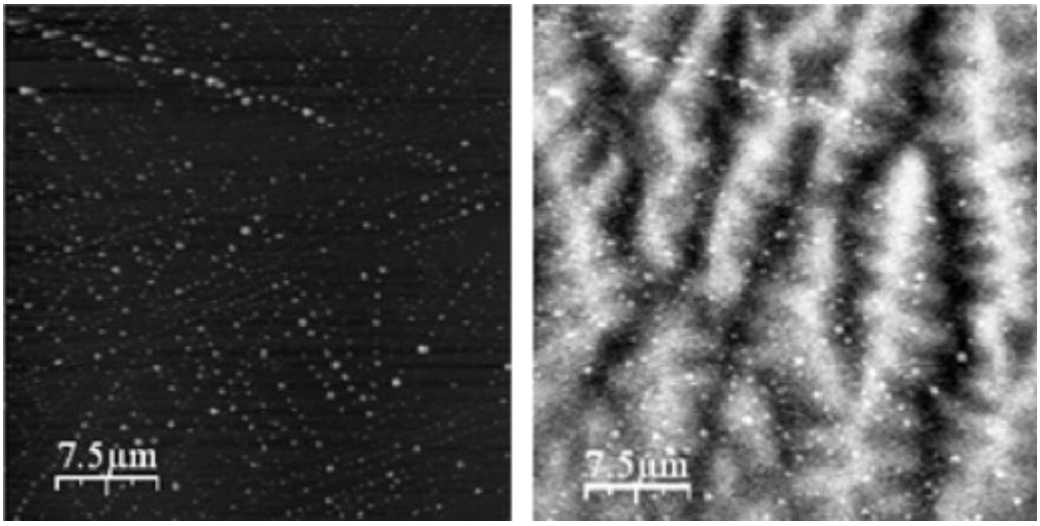

Figure 1. *Topography (left) and MFM (right) image of* $Fe_{40}Ni_{38}Mo_4B_{18}$ *ribbon without treatment.*

As shown in **Figure 2** and **Figure 3** the magnetic configuration changes from 90° domain walls to 180° domain walls when the treatment temperature is fixed at 450 °C for 1 h. At this temperature wider magnetic domains separated by thin 180° domain walls appear in the magnetic microstructure. In both cases, at 250 and 450 °C (for 1 h), the formed magnetic domain structure shows a regular magnetic domain configuration. Nevertheless, the microstructural change which takes place at these temperatures is very different: it has been mentioned that for the sample treated at 250 °C the internal stresses generated in the fabrication process have been released. In the sample treated at 450 °C the development of a nanocrystalline structure with a mean

grain size around 10 nm [18, 19] leads to a very low coercivity value that can be explained by the Herzer´s model [17] of random anisotropy.

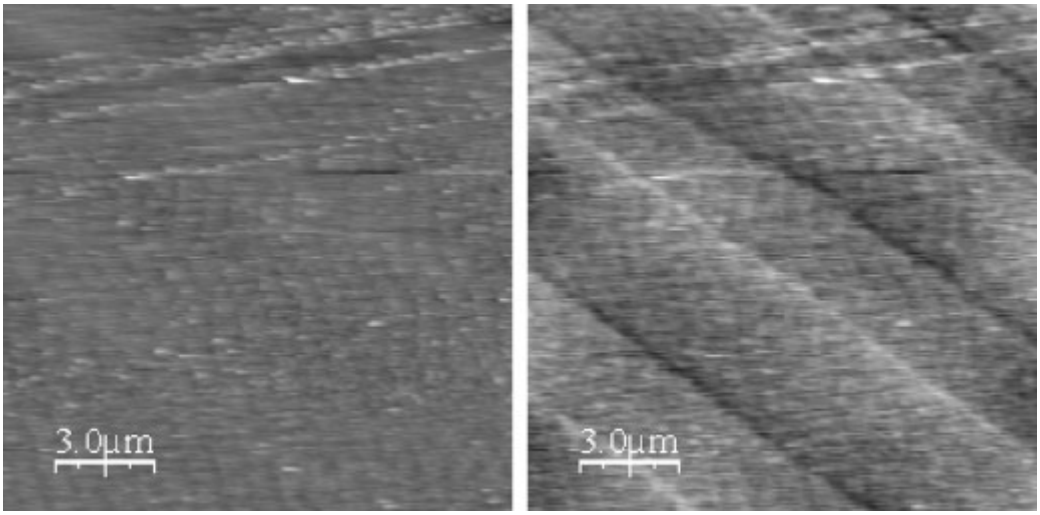

Figure 2. *Topography (left) and MFM (right) image of $Fe_{40}Ni_{38}Mo_4B_{18}$ ribbon after thermal treatment for 60 min at 250 °C. Topography scale: 173.2 nm. Magnetic scale: 1 V.*

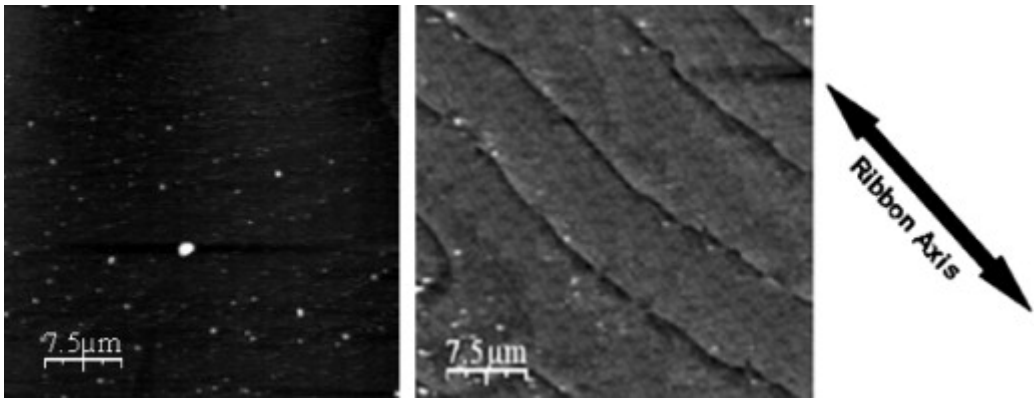

Figure 3. *Topography (left) and MFM (right) image of $Fe_{40}Ni_{38}Mo_4B_{18}$ ribbon after thermal treatment for 60 min at 450 °C. Topography scale: 114.8 nm. Magnetic scale: 2.3 V.*

At temperatures higher than 525 °C a crystalline phase of $Fe_{0.8}Ni_{0.2}$, which has a *fcc* crystal structure, appears. For the sample treated at 700 °C, the microstructure presents a large number of nanocrystalline particles in the amorphous matrix, as shown in the topography image (***Figure 4a***). Due to the crystallization process taking place in

the sample heat treated at 700 °C, the MFM image (***Figure 4b***) denotes the presence of hard magnetic (iron boride) grains with large value of magnetocrystalline anisotropy.

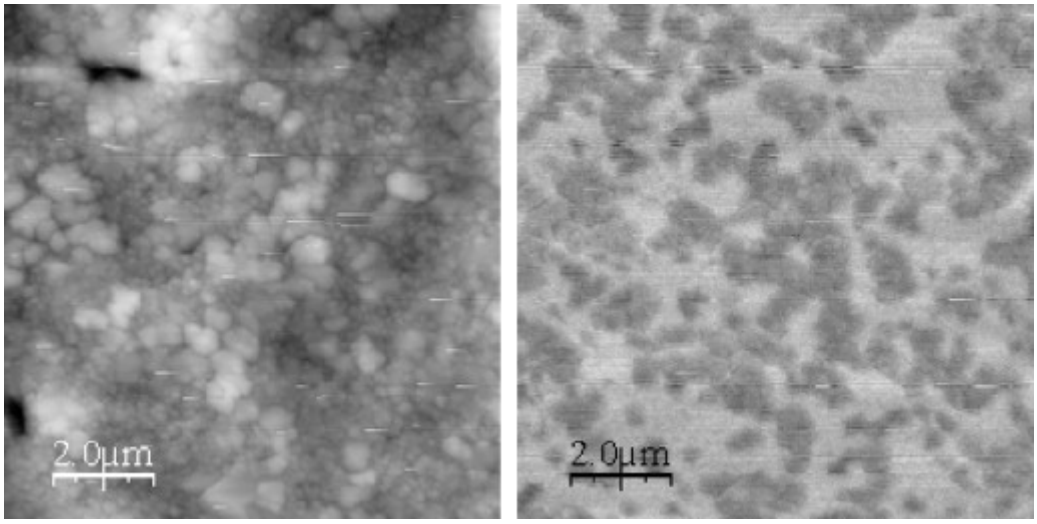

Figure 4. *Topography (left) and MFM (right) image of* $Fe_{40}Ni_{38}Mo_4B_{18}$ *ribbon after thermal treatment for 60 min at 700 °C. Topography scale: 361.3 nm. Magnetic scale: 3.8 V.*

3.2. Magnetic domains configuration in DC current treated samples.

The I_{DC} current flowing along the $Fe_{40}Ni_{38}Mo_4B_{18}$ ribbon axis generates a transverse magnetic field of inhomogeneous character [30] which can develop a transverse magnetic anisotropy being maximum at the surface ribbon. [12]

Figure 5 shows that the magnetic domains structure generated by current annealing gives rise to three different patterns depending on the treatment time: *labyrinths* and *zigzag* domains (1 A, 1 min), *zigzag* domains (1 A, 30 min) and *cells* (1 A, 1 h). At low treatment times both *zigzag* and *labyrinth* structures coexist in the magnetic structure. By increasing the treatment time, the regular *zigzag* domain structure dominates the magnetic structure. Finally, when the current treatment reaches 1 h, *cell* type domains structure appears in the magnetic domain structure. Depending on the requirements, different types of magnetic domains configuration can be obtained using a simple method like current annealing method. Several authors [12,13] have shown that this kind of treatment provokes drastic changes in magnetic behavior. An inhomogeneous magnetic anisotropy is lead and it is responsible for change in coercivity and in domains presented in this work.

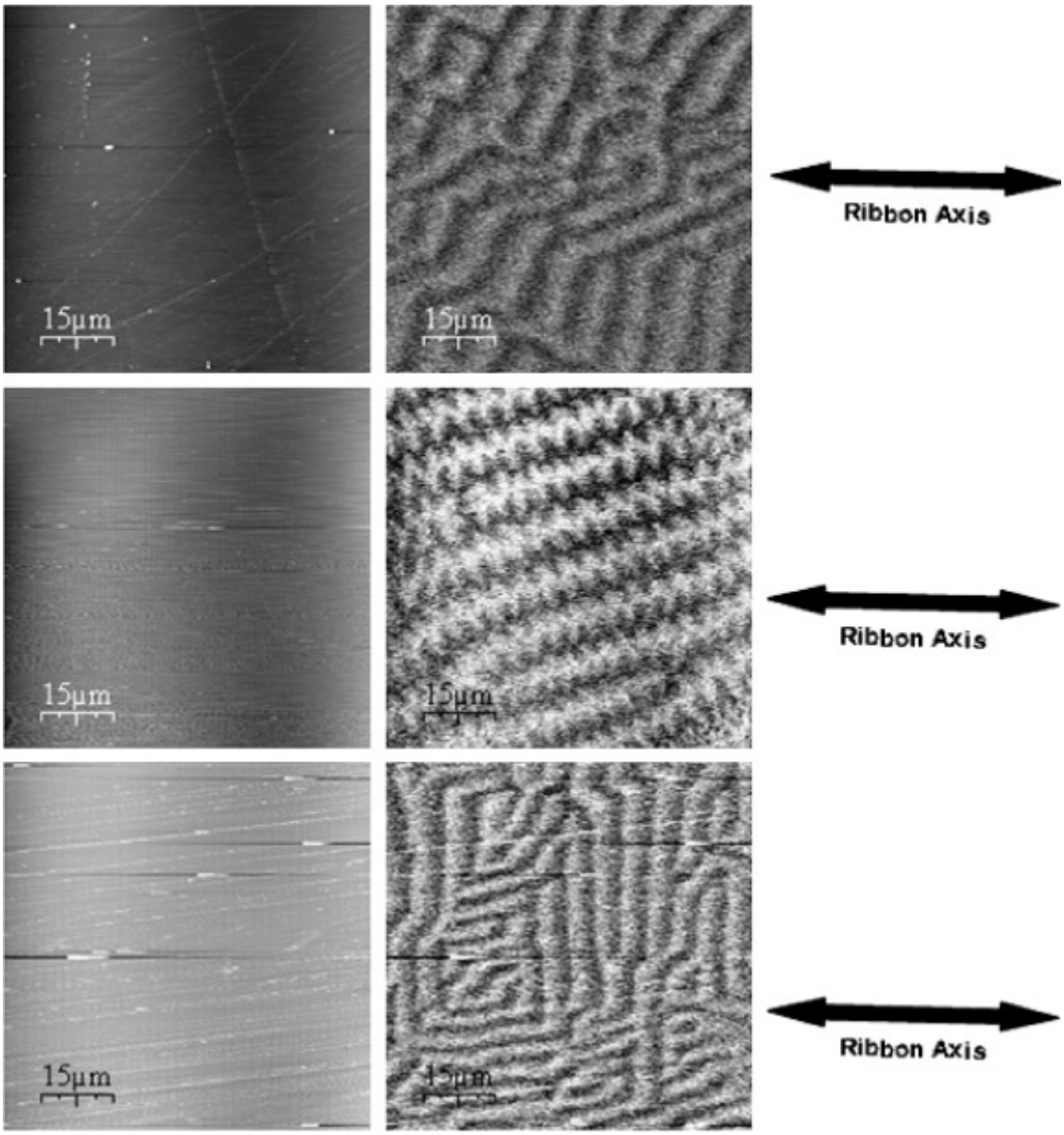

Figure 5. *Topography (left) and MFM (right) image of* $Fe_{40}Ni_{38}Mo_4B_{18}$ *ribbon after current treatment at 1 A for 1 min (a), 30 min (b) and 60 min (c). Topography scale: 100 nm. Magnetic scale: 135 mV.*

3.3. Magnetic domains configuration in simultaneous current and stress treated samples.

In general, different factors contribute to the total magnetic energy of a material, i.e., interactions with applied external magnetic fields, magnetocrystalline anisotropy, shape anisotropy, magnetostatic, magnetic exchange effects and stress anisotropy. [31] If a tensile or compressive force is applied to the sample during the thermal treatment, the

development of a macroscopic magnetic anisotropy, [32,33] one of the most important factors that determine the magnetic domain structure takes place. It is important to note that this stress-induced anisotropy is different from that induced by current[9] (section 3.2). The magnetic anisotropy induced by field or stress separately generates a different microstructure compared to the one obtained when the field and the stress are applied simultaneously. [32] In this case, the anisotropy depends on both composition and annealing parameters. The magnetic image of the stress annealed sample is shown in **Figure 6**. It is evident that the direction of the magnetic domains rotates and acquires the direction of the applied tensile stress owing to positive magnetostrictive character. The image of the compressed sample is shown in **Figure 7** in which *flower* magnetic domain structure appears and the magnetic domain direction is mainly perpendicular to the ribbon length axis. In addition, stress annealing can induce a transverse magnetic anisotropy, [33] in agreement with this MFM observation. The experimental results obtained coincide with the expected magnetic domain pattern in positive magnetostriction materials. In these materials, the magnetic domain's direction acquires mainly the direction of the traction axis.

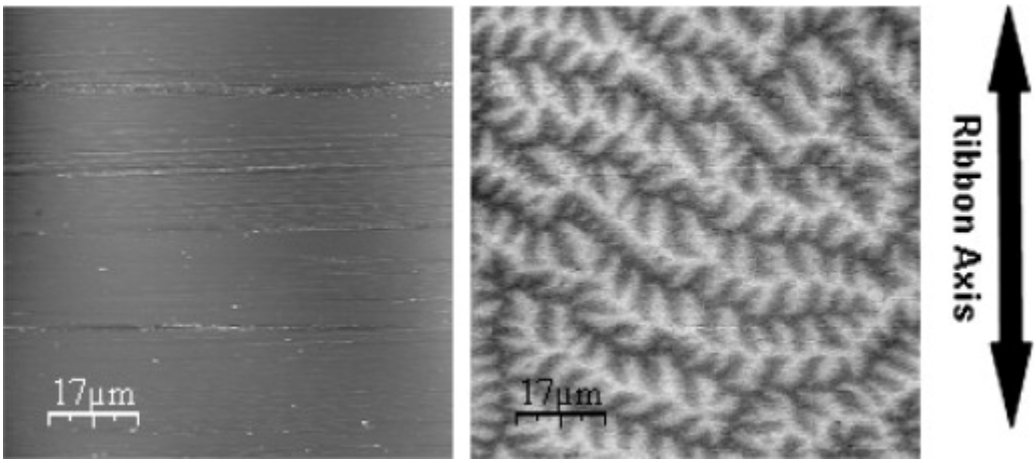

Figure 6. *Topography (left) and MFM (right) image of* $Fe_{40}Ni_{38}Mo_4B_{18}$ *ribbon after stress annealing treatment. Topography scale: 200 nm. Magnetic scale: 450 mV.*

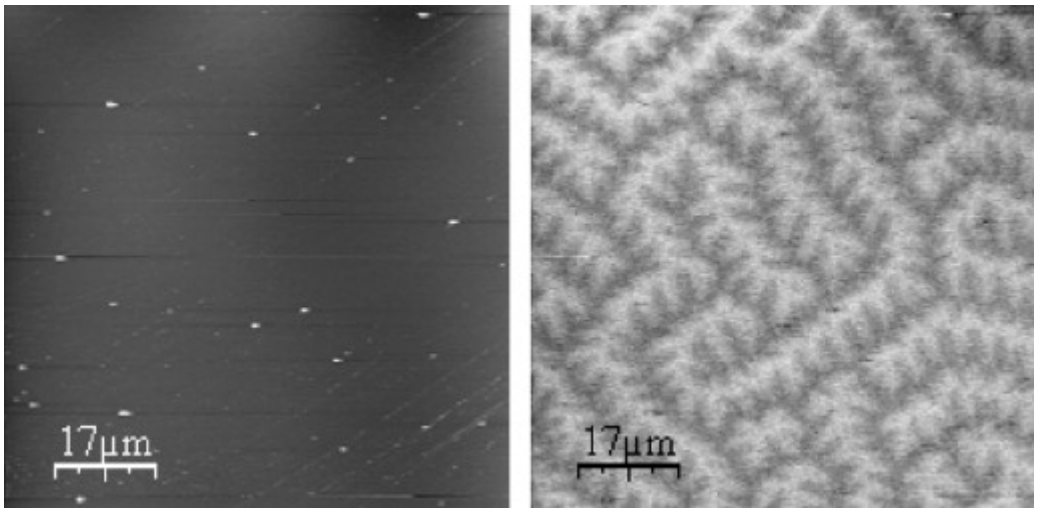

Figure 7. *Topography (left) and MFM (right) image of* $Fe_{40}Ni_{38}Mo_4B_{18}$ *ribbon after compression annealing treatment. Topography scale: 200 nm. Magnetic scale: 450 mV.*

4. Conclusions.

MFM characterization of soft magnetic amorphous alloy Metglas 2825MB thermally treated by conventional furnace and current annealing (with and without tensile stress) has been reported. The evolution of the domain structure surface is in agreement with the microstructural transformations associated with these kind of treatments, i.e., at low temperature (250 °C) the structural relaxation (via internal stress relief) leads to the disappearance of the maze domain.[30] Annealing at 450 °C provokes nanocrystallization [18,19] and the presence of a 180° domain wall, giving rise to a softer magnetic behavior. Strong crystallization (presence of large crystalline grains) is produced by the treatment of the sample at 700 °C.

Similarly, the current annealing method (without tensile stress) induces microstructural changes by increasing the time of treatment, while the current annealing with tensile stress develops a macroscopic transverse magnetic anisotropy of special interest for technological applications. In fact, this type of anisotropy is one of the requirements to observe giant magnetoimpedance effects.

Acknowledgement

The present work was supported by Ministerio de Educación y Ciencia (project MAT2007-66798-C03-01 and 03) and ETORTEK/NANOTRON project.

References

1. M. Tejedor, B. Hernando. Magnetic domains and anisotropy distribution in $Fe_{40}Ni_{40}P_{14}B_6$ amorphous ribbons. J. Phys. D: Appl. Phys., 13 (1980), 1709–1711.
2. C. Aroca, P. Sánchez, E. Lopez. Magnetoelastic effects in amorphous $Fe_{40}Ni_{40}P_{14}B_6$ alloys. IEEE Trans. Magn., 14 (1981), 1462–1467.
3. G. Riontino, M. Baricco. Structural relaxation in metallic glasses. Phil. Mag. B, 61 (1990), 715–725.
4. A. Van den Beukel. On the kinetics of structural relaxation in metallic glasses key. Eng. Mater., 81–83 (1993), 3–16.
5. M.R.J. Gibbs, J.E. Evetts, J.A. Leake. Activation-energy spectra and relaxation in amorphous materials. J. Mater. Sci., 18 (1983), 278–288.
6. E. Ascasibar, A. Hernando. Influence of structural relaxation on the magnetic-behavior of a metallic-glass. J. Phys. D: Appl. Phys., 18 (1985), L41–L47.
7. F.E. Luborsky, J.J. Becker, R.O. McCary. Magnetic annealing of amorphous alloys. IEEE Trans. Magn., 11 (1975), 1644–1649.
8. O.V. Nielsen. Separation into 2 contributions of stress anneal induced magnetic-anisotropy in metallic-glass ribbons. J. Magn. Magn. Mater., 36 (1983), 81–85.
9. J. González, M. Vázquez, J.M. Barandiarán, V. Madurga, A. Hernando. Different kinds of magnetic anisotropies induced by current annealing in metallic glasses. J. Magn. Magn. Mater., 68 (1987), 151–156.
10. T. Jagielinski. Flash annealing of amorphous-alloys. IEEE Trans. Magn., 19 (1983), 1925–1927.
11. A. Zaluska, H. Matyja. Rapid heating of Fe–Si–B metallic glasses. J. Mater. Sci. Lett., 2 (1983), 729–732.
12. M. Vázquez, J. González, A. Hernando. Induced magnetic-anisotropy and change of the magnetostriction by current annealing in co-based amorphous-alloys. J. Magn. Magn. Mater., 53 (1986), 323–329.
13. A.R. Yavari, R. Barrue, M. Harmelin, J.C. Perron. Rapid annealing of Fe–Si–B amorphous tapes by joule heating—effects on magnetic and mechanical-properties. J. Magn. Magn. Mater., 69 (1987), 43–52.
14. H.B. Van Veldhuizen, G.W. Koebrugge, J. Sietsma, A. Van den Beukel. The crystallization kinetics of amorphous $Fe_{40}Ni_{40}B_{20}$ measured by several physical-properties. J. Non-Cryst. Solids, 117/118 (1990), 240–243.
15. G. Wei, B. Cantor. The effect of heat treatment and surface treatment on the crystallisation behaviour of amorphous $Fe_{40}Ni_{40}B_{20}$. Acta Metall., 37 (1989), 3409–3424.

16. Y. Yoshizawa, S. Oguma, K. Yamauchi. New Fe-based soft magnetic alloys composed of ultrafine grain structure. J. Appl. Phys., 64 (1988), 6044–6046.
17. G. Herzer. Grain-size dependence of coercivity and permeability in nanocrystalline ferromagnets. IEEE Trans. Magn., 26 (1990), 1397–1402.
18. S.W. Du, R.V. Ramanujan. Crystallization and magnetic properties of $Fe_{40}Ni_{38}B_{18}Mo_4$ amorphous alloy. J. Non-Cryst. Solids, 351 (2005), 3105–3113.
19. R.V. Ramanujan, S.W. Du. Nanocrystalline structures obtained by the crystallization of an amorphous $Fe_{40}Ni_{38}B_{18}Mo_4$ soft magnetic alloy. J. Alloys Compd., 425 (2006), 251–260.
20. D. Rugar, H.J. Mamin, P. Guethner, S.E. Lambert, J.E. Stern, I. McFadyen, T. Yogi. Magnetic force microscopy—general-principles and application to longitudinal recording media. J. Appl. Phys., 68 (1990), 1169–1183.
21. K. Suzuki, D. Wexler, J.M. Cadogan, V. Sahajwalla, A. Inoue, T. Masumoto. Magnetic force microscopy study of nanocrystalline $Fe_{91}Zr_7B_2$ soft magnetic alloy. Mater. Sci. Eng. A, 226–228 (1997), 586–589.
22. A. Asenjo, M. Jaafar, D. Navas, M. Vázquez. Quantitative magnetic force microscopy analysis of the magnetization process in nanowire arrays. J. Appl. Phys., 100 (2006), 023909.
23. S.H. Liou, R.F. Sabiryanov, S.S. Jaswal, J.C. Wu, Y.D. Yao. Magnetic domain patterns of rectangular and elliptic arrays of small permalloy elements. J. Magn. Magn. Mater., 226–230 (2001), 1270–1272.
24. K. Watanabe, Y. Takemura, Y. Shimazu, J. Shirakashi. Magnetic nanostructures fabricated by the atomic force microscopy nano-lithography technique. Nanotechnology, 15 (2004), S566–S569.
25. T. Hysen, S. Deepa, S. Saravanan, R.V. Ramanujan, D.K. Avasthi, P.A. Joy, S.D. Kulkarni, M.R. Anantharaman. Effect of thermal annealing on $Fe_{40}Ni_{38}B_{18}Mo_4$ thin films: modified Herzer model for magnetic evolution. J. Phys. D: Appl. Phys., 39 (2006), 1993–2000.
26. M. Sorescu. Direct evidence of laser-induced magnetic domain structures in metallic glasses. Phys. Rev. B, 61 (2000), 14338–14341.
27. S.W. Du, R.V. Ramanujan. Characterisation of $Fe_{40}Ni_{38}B_{18}Mo_4$ nanomagnetic alloy. Mater. Sci. Eng. A, 375–377 (2004), 1040–1043.
28. A.P. Srivastava, D. Srivastaa, G.K. Dey. A study on microstructure, magnetic properties and kinetics of the nanocrystallization of $Fe_{40}Ni_{38}B_{18}Mo_4$ metglass. J. Magn. Magn. Mater., 306 (2006), 147–155.
29. J.D. Livingston. Stresses and magnetic domains in amorphous metal ribbons. Phys. Status Solidi (a), 56 (1979), 637–645.
30. A. Hernando, J.M. Barandiarán. Micromagnetics of twisted amorphous ribbons. Phys. Rev. B, 22 (1980), 2445–2449.
31. M.E. Hawley, G.W. Brown, D.J. Markiewicz, F. Spaepen, E.P. Barth. Magnetic force microscopy observation of the magnetic structure of deformation induced shear bands in amorphous $Fe_{80}B_{16}Si_4$. J. Magn. Magn. Mater., 190 (1998), 89–97.
32. J. González, K. Kulakowski. Stress and field induced magnetic anisotropies in Co-rich amorphous alloys. J. Magn. Magn. Mater., 82 (1989), 94–98.
33. J. González, J.M. Blanco, J.M. Barandiarán, M. Vázquez, A. Hernando. Basic Features of Glassy State. J. Colmenero, A. Alegria (Eds.). World Scientific Pb., Singapore (1990), p. 560.